

## Dynamic nuclear polarization at the edge of a two-dimensional electron gas

David C. Dixon, Keith R. Wald, and Paul L. McEuen

*Department of Physics, University of California at Berkeley, Berkeley, California 94720  
and Materials Sciences Division, E. O. Lawrence Berkeley National Laboratory, University of California, Berkeley, California 94720*

M. R. Melloch

*School of Electrical and Computer Engineering, Purdue University, West Lafayette, Indiana 47907*

(Received 8 January 1997)

We have used gated GaAs/Al<sub>x</sub>Ga<sub>1-x</sub>As heterostructures to explore nonlinear transport between spin-resolved Landau level edge states over a submicrometer region of two-dimensional electron gas (2DEG). The current  $I$  flowing from one edge state to the other as a function of the voltage  $V$  between them shows diodelike behavior—a rapid increase in  $I$  above a well-defined threshold  $V_t$  under forward bias, and a slower increase in  $I$  under reverse bias. In these measurements, a pronounced influence of a current-induced nuclear-spin polarization on the spin splitting is observed, and supported by a series of NMR experiments. We conclude that the hyperfine interaction plays an important role in determining the electronic properties at the edge of a 2DEG. [S0163-1829(97)06631-9]

### I. INTRODUCTION

The physics of two-dimensional electron gases (2DEG's) formed at GaAs/Al<sub>x</sub>Ga<sub>1-x</sub>As heterojunctions has become a very popular field in the past several years, owing to the 2DEG's many interesting properties, most notably the quantum Hall effect (QHE).<sup>1</sup> When placed in a strong perpendicular magnetic field, the electronic energy levels of the 2DEG congregate into Landau levels (LL's), whose energies are given by

$$E = \left( n + \frac{1}{2} \right) \hbar \omega_c + g \mu_B B S_z + E_{\text{ex}} + A \langle I_z \rangle S_z. \quad (1)$$

The first term of Eq. (1) gives the orbital LL splitting, where  $n$  is the orbital LL index and  $\hbar \omega_c$  is the cyclotron energy. The second term lifts the spin degeneracy of each orbital LL through the Zeeman interaction for GaAs,  $g \mu_B B \sim 0.016 \hbar \omega_c$ , with  $S_z$  being the electron spin ( $\pm \frac{1}{2}$ ). The third term expresses the effects of exchange, which depends sensitively on temperature and on the filling factor  $\nu = n_s \hbar / eB$  (the number of LL's filled for 2D electron density  $n_s$ ). Exchange can affect the total energy considerably, sometimes by as much as a few meV. The final term involves the influence of nuclear polarization  $\langle I_z \rangle$  through the contact hyperfine interaction, the effect of which is the focus of our paper and is discussed in more detail later.

Due to their high mobility and ease of fabrication, 2DEG's provide a useful medium for examining many-body physical effects, such as exchange. Even though the Zeeman energy splitting is only a tiny fraction of the orbital LL splitting, exchange effects favor a ferromagnetic ground state near  $\nu = 1$ , increasing the effective spin gap. It has recently been observed that the low-energy excitations of such a spin-polarized 2DEG are not single spin flips, but rather spatially extended spin textures (skyrmions), in which electrons gradually tilt their spins from the center of the texture outward, with the size of the skyrmion set by the competition

between exchange and Zeeman energies.<sup>2</sup> Skyrmions have been detected using various techniques<sup>3,4</sup> in bulk 2DEG's, underscoring the importance of treating the 2DEG as an interacting many-body system.

It is recognized that the *nuclei* of the GaAs crystal can affect the electronic properties of the 2DEG as well. Any nonzero nuclear polarization  $\langle I_z \rangle$  will create an extra effective magnetic field felt by the electrons, producing an Overhauser shift in the electron energies that can be detected with electron spin resonance absorption.<sup>5</sup> In turn, a net electron polarization produces a Knight shift in the nuclear energies, which can be used to measure the spin polarization of the 2DEG.<sup>3</sup> In addition to these energy shifts, the hyperfine interaction allows "flip-flop" scattering in GaAs, where an electron "flips" its spin simultaneous with the "flop" of a nuclear spin in the opposite direction, conserving the net spin of the entire system.

Nuclear spin effects in bulk 2DEG's have been well-studied, but in this paper we shall be examining these effects at the edge of the 2DEG. When  $\nu$  is an integer, all occupied LL's are full and the bulk 2DEG is incompressible. At the edge, however, the electron density gradually descends from  $\nu$  to zero and the LL energies curve upward, due to the electrostatic confinement potential. The intersections of the LL's with the Fermi energy  $E_F$  near the edge define regions where electrons can be added to the 2DEG. These "edge states" (or "edge channels") are spatially separated independent channels, each carrying an identical amount of current at equilibrium.<sup>6</sup> Self-consistent electrostatic screening modifies the edge states, creating wide compressible and incompressible stripes at the edge, with a corresponding step-like potential profile [Fig. 2(a)].<sup>7-11</sup>

The complete many-body physics of the edge is not well understood, although theories predict that the edge may exhibit many-body phenomena, such as spin textures.<sup>12</sup> The relative tininess of the edge region makes many measurement techniques unfeasible, but electronic transport, which necessarily takes place at the edge in the QH regime, pro-

vides a probe into the nature of these states. At equilibrium the edge states all maintain the same electrochemical potential. Using submicrometer gates deposited on top of the heterostructure, however, one can selectively backscatter the edge states, induce different potentials in different edge states, and measure the resultant interedge scattering.<sup>13</sup> Scattering between spin-degenerate<sup>14</sup> and spin-split<sup>15</sup> edge states has been considered previously for the linear regime, as has nonlinear scattering between spin-degenerate edge states.<sup>10,16</sup> In this paper, we report measurements of nonlinear transport between spin-split edge states, and show that spin-flip relaxation produces a nuclear polarization of the Ga and As nuclei. This polarization can in turn drastically affect the electronic energies at the edge of a 2DEG.

In Sec. II of this paper, we describe the measurement setup and the method by which a potential imbalance is created between spin-split edge states using submicrometer gates. We also describe a simple picture of the edge utilizing the “spin diode” model used by Kane *et al.*<sup>17</sup> Section III contains our experimental results, which display features that are best explained by dynamic nuclear polarization (DNP) of the nuclear spins. We present strong evidence for this interpretation with a series of NMR experiments. We continue in Sec. IV with some observations about the data, and we briefly discuss some possible consequences of our results for models of the spin-split edge. In Sec. V we compare our findings with earlier results by our group,<sup>18</sup> and we conclude in Sec. VI.

## II. MEASUREMENT METHODOLOGY

A schematic diagram of the device under consideration is shown in Fig. 1(a). Electrons populated up to an electrochemical potential  $\mu = -eV$  enter the two spin-split edge channels from contact 1. Gates A and B (“AB split-gate”) are tuned so that the upper (inner, spin-down) edge state is reflected by the gate’s potential barrier, but the lower (outer, spin-up) channel is transmitted. After passing through these gates, the outer edge channel, still at potential  $\mu$ , propagates along gate A in close proximity to the grounded inner edge channel. The edge channels are not in equilibrium in this region, so there is a net scattering of electrons from one channel to the other. These scattered electrons propagate in the inner edge channel to a current amplifier (contact 3) and are measured as current  $I$ . Unscattered electrons remain in the outer edge channel and pass between gates A and C (“AC split-gate”) into the grounded contact 2 and avoid detection by the current amplifier. The current  $I$  measured in this three-terminal arrangement therefore solely originates from interedge scattering.

One may notice in Fig. 1 that the outer edge states are shown going underneath gates B and C. This is because these gates are only partially depleted, but depleted enough so that the electron density beneath the gate is such that only one LL is filled ( $\nu \sim 1$ ), and the inner (spin-up) edge state is reflected. The region of 2DEG between the split gates must also reflect the inner edge state, which can be accomplished by increasing the voltage on gate A ( $V_A$ ) to partially deplete the 2DEG to  $\nu \sim 1$  throughout this region. The reasons for using this semidepletion method are detailed in Sec. V.

A schematic electrochemical energy diagram of the

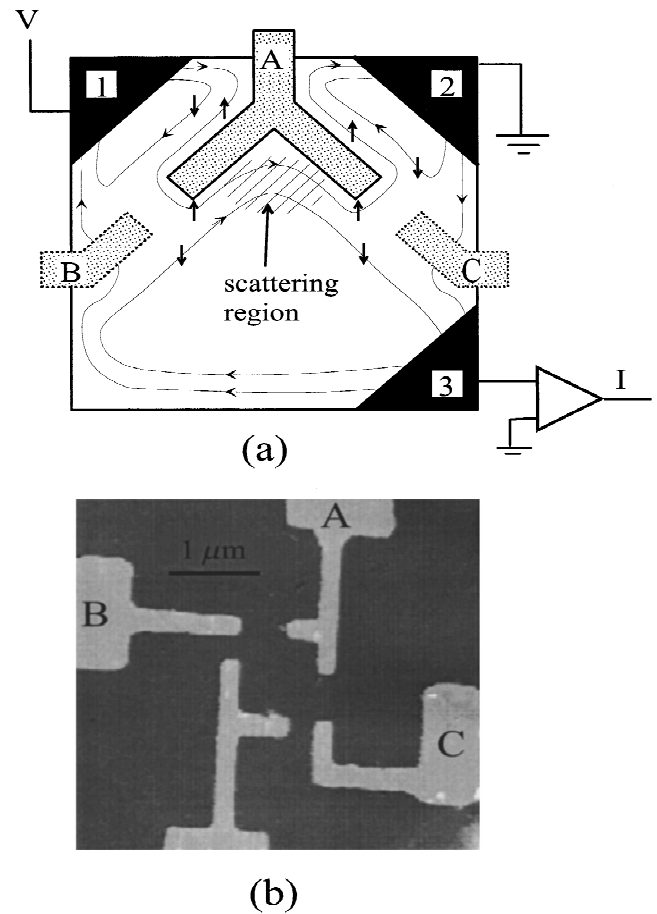


FIG. 1. (a) Schematic of device geometry for filling factor  $\nu=2$ . Electrons of both spins enter from contact 1 at a bias  $V$ . Only the spin-up edge channel is transmitted through gates A and B, and the electrons in this edge channel enter the scattering region where they can scatter into the grounded spin-down edge channel. Scattered electrons then proceed to the current amplifier attached to contact 3 (lower right) and are measured as current  $I$ . Unscattered electrons disappear into the grounded contact 2 (upper right) and avoid detection. (b) AFM image of the device, with a 1  $\mu\text{m}$  bar provided as a reference. The bottom gate was not used in these experiments, so it was grounded.

2DEG edge is shown in Fig. 2, where the bulk of the sample is to the left and the edge is to the right. A combination of the sample’s electrostatic confinement potential and the electrons’ ability (or inability) to screen this potential leads to the slanting stepwise energy profile shown.<sup>9</sup> Electrons in the compressible regions can move around to screen the external confinement potential, creating the energetically flat regions shown. The electron density within each compressible strip falls steadily from left to right. Between the compressible regions, the electron density is fixed at integer filling factor, so these incompressible regions cannot screen the confinement potential. It should be noted that this picture does not include quantum mechanical electron-electron interactions such as exchange, which complicate the picture considerably. We will discuss this complication in Sec. IV.

The energy level diagram in Fig. 2 resembles that of a diode,<sup>17</sup> with the spin-split edge states playing the role of the diode’s  $p$ - and  $n$ -doped regions. When the outer edge channel is forward biased, as shown in Fig. 2(b), the energy dif-

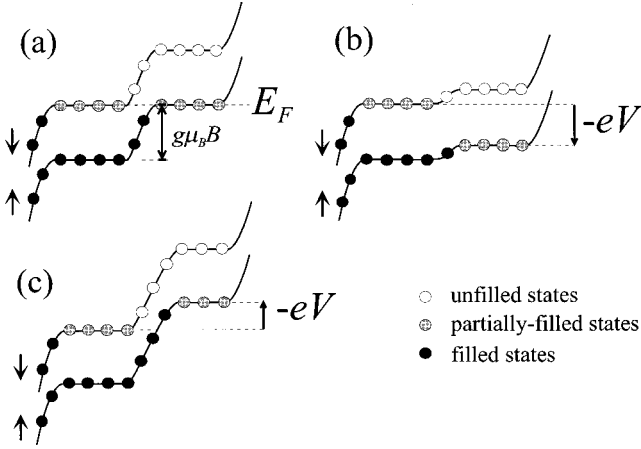


FIG. 2. Landau level energy diagram near the edge of a 2DEG, for no bias (a), forward bias (b), and reverse bias (c). The electron energies flatten out at the Fermi energy  $E_F$  due to self-consistent electrostatic screening, forming compressible strips (flat regions, gray dots) and incompressible strips (sloped regions, black dots). In forward bias (b), very little current flows unless  $eV$  exceeds  $g\mu_B B$ , whereupon electrons can move readily from the inner to the outer edge channel. In reverse bias (c), the current consists only of electrons that tunnel through the incompressible strip from the outer to the inner edge channel.

ference between the partially filled states of the inner edge channel and the available empty states of the outer edge channel decreases, and the incompressible strip between the edge channels becomes narrower.<sup>19</sup> For small forward bias, only a small current of thermal electrons will flow between the edge states, resulting in a small  $I$ . Once  $|eV|$  exceeds the LL energy splitting  $g\mu_B B$ , however, the incompressible strip disappears, and a large current of electrons can move freely from the inner to outer edge channels. We therefore expect a threshold voltage  $V_t$  in the  $I$ - $V$  trace, corresponding to the LL energy splitting. Conversely, for negative bias [Fig. 2(c)], the interedge energy splitting becomes enhanced, and in order to scatter between edge states, electrons must tunnel through the incompressible strip, leading to a small  $I$  which depends on both the bias  $V$  and the width of the tunnel barrier (which is itself a function of  $V$ ). Because of the different modes of transport for forward and negative bias, there should be an asymmetry in  $I$ . Previous experiments on transport between large compressible regions<sup>17,19,20</sup> and between spin-degenerate edge channels and large compressible regions<sup>21</sup> have shown this asymmetry.

Since the LL's in the spin diode are of opposite spin, the scattering of an electron from one LL to the other must be accompanied by a spin flip. It is important to note, however, that for forward bias, electrons do not necessarily have to flip their spins in order to register a current  $I$ . They can be excited from the upper LL of the inner edge channel (thermally, or with help from a high bias) into the empty states in the upper LL of the outer edge channel, and stay in that channel long enough to make it through the  $AC$  split gate and disappear into contact 2. However, some of these ‘‘hot’’ electrons in the upper LL relax to the lower LL by flipping their spin, which can be caused either by spin-orbit scattering<sup>15</sup> or by the contact hyperfine interaction between

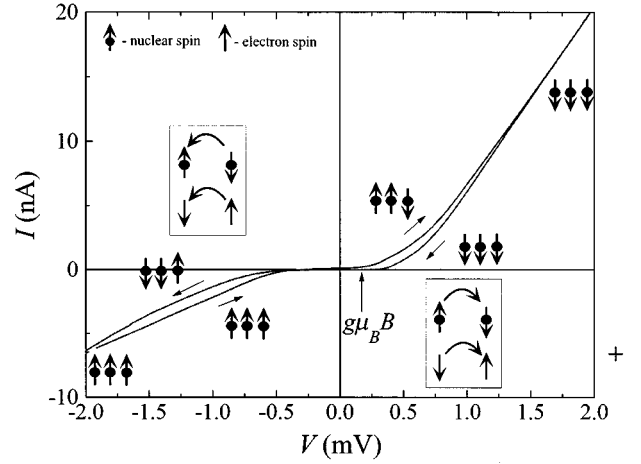


FIG. 3. Spin diode  $I$ - $V$ . For forward bias, the current is small until  $-eV$  reaches a threshold voltage comparable to the bare spin splitting  $g\mu_B B = 0.175$  meV. In reverse bias, the current gradually increases with no apparent threshold. The trace also displays hysteresis, with the  $V$  sweep direction indicated by the arrows. The two insets schematically show the flip-flop scattering between electron spins and nuclear spins for negative and positive bias. The nuclear polarization is schematically shown for each step of the hysteresis loop, as discussed in the text.

the electron and the Ga and As nuclei.<sup>22</sup> We will be concerned with the effects of this hyperfine-mediated scattering.

### III. EXPERIMENTAL RESULTS AND INTERPRETATION

The device was fashioned from a GaAs/Al<sub>x</sub>Ga<sub>1-x</sub>As heterostructure with a 2DEG density  $n_s = 2.5 \times 10^{11}$  electrons/cm<sup>2</sup> and a mobility of  $\sim 10^6$  cm<sup>2</sup>/Vs. Patterned split gates of layered Cr and Au were evaporated on the surface of the structure, and Ni/Ge/Au contacts were annealed to make electrical contact with the 2DEG. The device is shown in Fig. 1(b). The current measurement setup used a virtual-ground preamplifier in a standard dc configuration, with the device mounted in a dilution refrigerator and cooled to a base temperature of 30 mK.

For all the spin diode experiments, the magnetic field was set to 7.0 T ( $\nu=2$ ) and the  $AC$  and  $AB$  split gates were tuned to transmit only the outermost edge state, as shown in Fig. 1(a), so that the measurement probes the scattering between  $n=0\uparrow$  and  $n=0\downarrow$  Landau levels. A typical  $I$ - $V$  measurement is plotted in Fig. 3, showing a rapid increase of current in forward bias with a more gradual increase in reverse bias, as predicted by the spin diode model described in Sec. II. Note that the forward-bias threshold voltage  $V_t$ , where  $I$  rapidly changes slope, is comparable to, but greater than, the bare spin splitting  $g\mu_B B \sim 0.18$  meV. This is much less than the exchange-enhanced spin splitting (a few meV) in the bulk 2DEG. We will return to this in Sec. IV.

We did not observe the complex structure under reverse bias reported by Kane *et al.*,<sup>17</sup> possibly because our device has a different geometry than the interrupted Corbino-style device used in their experiments. Also, as we will show in the Discussion section, the estimated width of the incompressible region in the Kane spin diodes (70 nm) is about ten times larger than ours, and as such could be large enough to

exhibit different many-body effects than what we observe.

An important observation is that the  $I$ - $V$  curve in Fig. 3 is hysteretic. The direction of the hysteresis is indicated by the arrows. For forward bias, the current is larger sweeping up in bias than when sweeping down, and for negative bias, the current is more negative sweeping up towards zero bias than when sweeping down away from zero bias. The size of the hysteresis loop depends on the sweep rate; the sweep shown in Fig. 3 lasted approximately five minutes. If the sweep is halted at some point in the loop, the current exponentially<sup>23</sup> relaxes to an equilibrium value with a long relaxation time, typically on the order of 30 seconds.

To understand the origin of this hysteresis, we first note that the equilibration time constant is similar to previously measured nuclear relaxation times for Ga and As in quantum wells,<sup>24</sup> indicating that the source of the hysteresis is the influence of the GaAs nuclear spins upon the 2DEG electron spin energies through the contact hyperfine interaction. The hyperfine Hamiltonian is

$$A\vec{I}\cdot\vec{S}=\frac{A}{2}(I^+S^-+I^-S^+)+AI_zS_z, \quad (2)$$

where  $A$  is the hyperfine constant, and  $\vec{I}$  and  $\vec{S}$  are the nuclear and electron spins, respectively. The first term of Eq. (2), consisting of ladder operators, corresponds to the simultaneous flip flop of electron and nuclear spins, and the second term is the hyperfine splitting.

We connect the hysteresis of Fig. 3 to the hyperfine interaction as follows. In our experiments a steady influx of spin-polarized electrons enters through the  $AB$  split gate, dynamically polarizing the nuclei in the scattering region through flip-flop scattering. The formation of a nuclear polarization  $\langle I_z \rangle$  in turn affects the electron energies through the Zeeman-like term  $A\langle I_z \rangle S_z$ , which acts like an effective magnetic field  $B_{\text{eff}}=\langle I_z \rangle/g\mu_B$  (Overhauser effect). This extra field changes the LL energy splitting to  $g\mu_B(B+B_{\text{eff}})$ , which in turn shifts the threshold voltage  $V_t$ . Let us consider that the voltage  $V$  begins at large negative bias (lower left-hand corner of Fig. 3). Here the current flow is from outer to inner edge states, which involves a spin flip of up to down. This spin flip, through the hyperfine interaction, ‘‘flops’’ a nucleus from ‘‘down’’ to ‘‘up,’’<sup>25</sup> so a steady current flow results in a net spin-up nuclear polarization (positive  $\langle I_z \rangle$ ). When  $V$  is swept up to positive values, the spin diode is in forward bias, so that a large current will begin to flow from inner to outer edge states once  $V$  reaches the threshold voltage  $V_t$ . This threshold, however, is not just the bare spin splitting  $g\mu_B B$ ;  $\langle I_z \rangle$  is still nonzero because of the slow nuclear polarization decay rate, and it creates a negative  $B_{\text{eff}}$  ( $g=-0.44$ ). Therefore,  $V_t$  is lowered and  $I$  is increased, compared to the case of unpolarized nuclei. Continuing the sweep, at large positive bias the current is from inner to outer edge states, which can involve a spin flip from down to up. This ‘‘flops’’ a nucleus from ‘‘up’’ to ‘‘down,’’ so a steady current flow in this case pumps the nuclei towards a net spin-down nuclear polarization (negative  $\langle I_z \rangle$ ). A negative  $\langle I_z \rangle$  creates a positive  $B_{\text{eff}}$ , which increases  $V_t$  and decreases  $I$ . This accounts for the lower branch of the hysteresis loop for forward bias in Fig. 3. To finish the sweep,  $V$  goes back

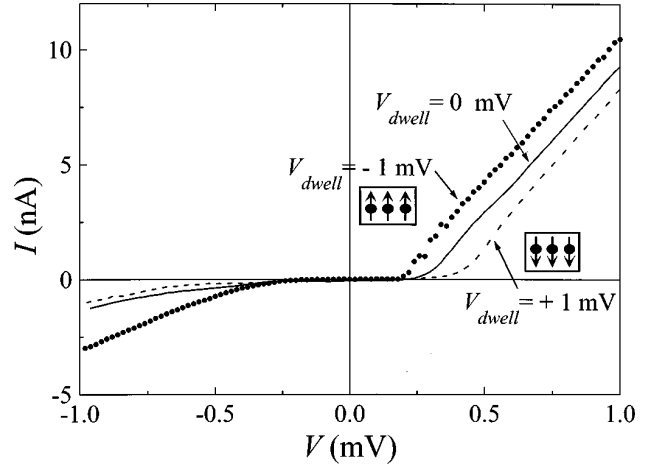


FIG. 4.  $I$ - $V$  traces taken at constant nuclear polarization. For each trace, the nuclei were prepared by dwelling at a specified voltage  $V_{\text{dwell}}$  for 60 sec, then quickly changing the voltage to another value, measuring  $I$ , and returning to  $V_{\text{dwell}}$  to maintain the polarization. For  $V_{\text{dwell}}=-1$  mV, the nuclear polarization was up, and for  $V_{\text{dwell}}=+1$  mV, the polarization was down. The threshold voltage is shifted by the Overhauser effect of the prepared nuclear polarization on the electrons.

to negative values, the current flow pumps the nuclei back to a spin-up polarization, and the cycle repeats.

The important point of this model is that the current induces a nuclear polarization through the flip-flop term of Eq. (2), and is in turn affected by the already-existing nuclear polarization through the Zeeman term of Eq. (2). The complex interplay between the two effects, combined with the long relaxation times for Ga and As nuclei, leads to the observed hysteresis.

It would be useful to observe these hyperfine effects independently of each other by measuring the  $I$ - $V$  profile of the spin diode at a constant  $\langle I_z \rangle$ . To do this, we performed experiments where we held  $V$  at a fixed value  $V_{\text{dwell}}$  for 60 sec—long enough for  $\langle I_z \rangle$  to reach equilibrium—then quickly ramped  $V$  to a voltage, measured  $I$  at that voltage, and immediately returned to  $V_{\text{dwell}}$  to reset the nuclear polarization. This small duty cycle procedure, repeated for many values of  $V$ , keeps the system in a state of constant nuclear polarization, while measuring the  $I$ - $V$  profile at this fixed polarization. Similar experiments were carried out by Kane *et al.*<sup>17</sup>

Three examples of these measurements, for  $V_{\text{dwell}}=+1$ , 0, and  $-1$  mV, are shown in Fig. 4. According to the model, these  $I$ - $V$ 's should correspond to an enhancement, no effect, and a decrease in the electron spin splitting, respectively. This is indeed what is observed, seeing that  $V_t$  is shifted by a significant amount between dwell plots as being the Overhauser shift. For  $V_{\text{dwell}}=0$  mV, we believe the nuclei remain unpolarized, and the threshold  $V_t\sim 0.27$  mV. This suggests that  $g$  is slightly enhanced ( $g^*\sim 1.5g$ ), yet still much smaller than has been measured in bulk 2DEG's,<sup>26,27</sup> where  $g^*$  can be as large as  $20g$ . We interpret the shift  $\Delta V_t$  between dwell plots as being the Overhauser shift. For both  $V_{\text{dwell}}=+1$  V and  $-1$  V,  $e|\Delta V_t|=A\langle I_z \rangle S_z\sim 0.10$  meV, corresponding to an effective Overhauser field of about 4 T. The maximum Overhauser

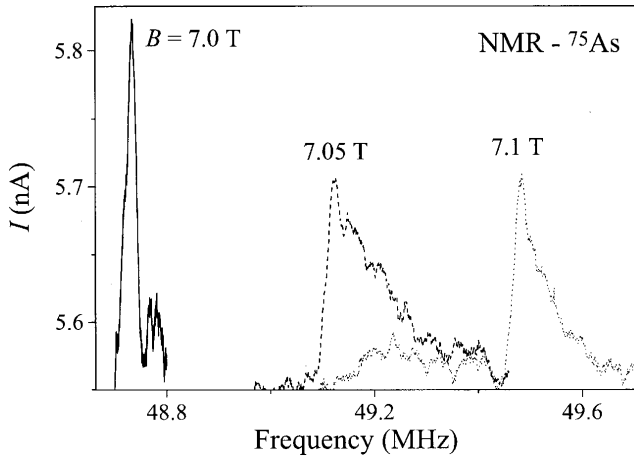


FIG. 5. NMR absorption peaks, showing a marked change in current when the frequency of an in-plane ac magnetic field matches the splitting of a nuclear species (in this case,  $^{75}\text{As}$ ). The peaks shift linearly with  $B$ . All plots were taken sweeping frequency from left to right. The  $B=7.0$  T peak was swept at a much slower rate than the other two peaks, which have asymmetric line shapes because the sweeping rate was comparable to the equilibration rate of nuclear repolarization.

field for GaAs (Ref. 27) is 5.3 T, so the nuclear spins in the scattering region must be highly polarized (about 85%).

To demonstrate further that  $I$  is indeed affected by the state of the nuclear spins, we performed a series of NMR experiments with the spin diode. We mounted a simple one-turn coil next to our sample, to which we applied a frequency-tunable ac voltage in order to produce an ac magnetic field perpendicular to  $B$  (i.e., in the plane of the 2DEG). The spin diode was held at forward bias  $V_{\text{dwell}} > V_t$ , polarizing the nuclei in the scattering region. Figure 5 displays  $I$  as a function of coil frequency near the  $^{75}\text{As}$  resonance, for three slightly different values of  $B$ . For all measurements, the frequency was swept from low to high values. Each trace shows a well-defined peak in current, with the peak shifting to higher frequencies for increasing  $B$ .

The peaks are due to NMR absorption; matching the in-plane ac magnetic field frequency to the NMR absorption energy for a nuclear species partially erases the polarization of that species, decreasing the Overhauser shift (and  $V_t$ ) and leading to a sudden increase in current. The peak is located at the expected NMR frequency for  $^{75}\text{As}$ , and scales appropriately with  $B$ . Similar behavior was seen for the  $^{69}\text{Ga}$  and  $^{71}\text{Ga}$  absorption lines.<sup>28</sup> Kane *et al.*<sup>17</sup> reported similar NMR results in their spin diode experiments.

The long exponential tail on the right side of the peaks for  $B=7.05$  and  $7.1$  T is due to the long equilibration time, which was comparable to the frequency sweeping rate in these measurements. The  $B=7.0$  T peak was swept much more slowly, so that the nuclei were always close to equilibrium during the sweep, as evidenced by the disappearance of the long tail. When the ac frequency is swept very slowly, the widths of the NMR features are approximately 20 KHz. This is on the order of the Knight shift expected for the electron density of our 2DEG,<sup>29</sup> and we will discuss this further in the next section.

We carried out a series of similar diodelike experiments at

$\nu=4$ , measuring scattering between spin-degenerate orbital LL edge states. In those experiments, we observed asymmetric  $I$ - $V$  curves with a threshold voltage  $V_t$  comparable to the cyclotron energy  $\omega_c = eB/m^*$ . More details about these experiments are published elsewhere.<sup>30</sup>

#### IV. DISCUSSION

We first note that, although our simple model of the spin-split edge explains the electron transport data rather well, it does not include the well-documented effects of exchange, which have been observed<sup>26</sup> to greatly increase the spin gap in bulk 2DEG's near  $\nu=1$ . These effects have been predicted to manifest themselves at the edge as well, particularly in the neighborhood of the  $\nu=1$  incompressible strip. One theory of the spin-split edge<sup>31</sup> predicts that the spin gap in this region can be enhanced by as much as a factor of 50. Our measurements of this gap (through the threshold voltage  $V_t$ ) appear to indicate otherwise—the spin gap is only slightly enhanced ( $g^* \sim 1.5g$ )—but this conclusion is based upon the assumption that  $V_t$  and  $g^* \mu_B B$  are directly related.

To estimate the various pertinent length scales, we applied the self-consistent electrostatic model of Chklovskii *et al.*<sup>9</sup> to spin-split edge states, substituting the bare spin gap  $g \mu_B B$  for  $\hbar \omega_c$ . In this case, the  $\nu=1$  incompressible strip is centered at about 70 nm from the edge of the 2DEG, with a width of about 7 nm, comparable to the magnetic length  $\lambda$  (10 nm). At length scales this small, the local density approximation fails, so it is reasonable to expect that exchange calculations for bulk samples cannot be applied directly to such a small edge region. More sophisticated theories of the physics of spin-split edge states do exist, and we discuss their relevance to our experiments as follows.

One theory<sup>31</sup> of spin-split edge states predicts hysteresis due entirely to electron-electron interactions. At a critical potential imbalance  $\Delta \mu_{\text{cr}}^+$ , the edge channels are predicted to switch positions, remaining in this switched orientation until a different potential difference  $\Delta \mu_{\text{cr}}^-$  is reached. We believe, however, that our DNP interpretation explains the observed hysteresis adequately, and we see no compelling evidence of this channel-crossing phenomenon. Another theory<sup>12</sup> predicts that, for certain ranges of the depletion width  $w$  (normalized to  $\tilde{w} = w/\lambda$ ) and Zeeman strength  $\tilde{g} = g \mu_B / (e^2/e\lambda)$ , the 2DEG edge supports spin deformations running along the edge (for  $\nu < 1$ ). We estimate our device's parameters to be  $\tilde{w} \sim 7$  and  $\tilde{g} \sim 0.016$ , placing it within the parameter space where these spin-textured edges are predicted to exist. This textured edge theory, however, makes no predictions about the transport properties of such a system, so we cannot confirm the existence of such a texture in our experiment. We know of no theory which specifically predicts the current flow between spin-split edges as a function of the nonlinear potential difference between them. Such a theory would require careful examination of many different facets of the problem: self-consistent electrostatics, exchange interactions, potential imbalances, electrodynamic effects due to interedge current flow, and, as we discuss below, hyperfine interactions.

It is clear from the dwell plots in Fig. 4 that a net nuclear polarization creates a large Overhauser shift of the edge-state

energies, so we believe that a complete description of the physics of the 2DEG edge cannot ignore hyperfine effects. While it is true that edge-state transport experiments in the linear regime (i.e.,  $|eV| < g\mu_B B$ ) will not create a nuclear polarization, it is clear from our experiments that nonlinear transport between spin-split edges can create one, so it is important to consider hyperfine effects in this regime. The many-body effects predicted by theory could very well be affected by the nuclear polarization, adding yet another complication to the spin-split 2DEG edge model. Although the inclusion of the hyperfine interaction appears to just complicate an already complicated model, it might actually be useful as a tool for measuring the spatial electron spin variation.

As we have shown, the Overhauser shift can provide information about the local nuclear polarization, so it seems possible that the Knight shift can likewise be used as a probe of the spatially varying electron spin density near the edge. At  $\nu=2$  the bulk of the 2DEG produces no Knight shift, since the net electron spin is zero. Near the edge, however, there will be a region (the incompressible strip) of only one spin species, fringed by regions of unbalanced spin mixtures. These regions of 2DEG would produce Knight shifts due to their net electron spin. The summation of the Knight shifts from different regions of spin density should produce overstructure on the NMR absorption peaks. Some of our data (not shown) show asymmetric NMR peaks with a slight bump on the left side, where a Knight-shifted peak would be expected to appear. Unfortunately, due to the switching noise of our sample, we were unable to accurately measure this overstructure, but we plan to pursue this method in the near future.

## V. COMPARISON WITH OUR EARLIER EXPERIMENTS

The experiments outlined in this paper are continuations of previous work by our group<sup>18</sup> examining DNP effects using a similar experimental setup.<sup>32</sup> In this section, we review those previous results, noting that the observed hysteresis differed in important ways from the results reported in Sec. III. We then discuss the origin of the differences between the two experiments. We show that the voltages on the gates must be carefully chosen if they are to properly inject and detect the spin-polarized edge currents. In the experiments of Ref. 18, this was not done, leading to what we now believe is an incorrect interpretation of the relative importance of the flip-flop and Zeeman terms in the experiments. In particular, the hysteresis in Ref. 18 was attributed entirely to the effects of flip-flop scattering, while we now feel that the influence of the nuclear Zeeman term was crucial to understand the experiments.

In the experiments of Ref. 18, the  $I$ - $V$  curves displayed *symmetric* hysteresis. By this we mean that  $|I|$  was greater when  $V$  was being swept away from zero than it was when being swept toward zero, for both positive and negative  $V$ . In other words, starting from the origin and sweeping  $V$  from zero to (say)  $+1$  mV to  $-1$  mV to zero, the absolute current values were, in sequence: high, low, high, low. We explained this hysteresis by considering the currents carried by flip-flop scattered electrons. Whenever the voltage changes sign, inter-edge scattering increases due to flip-flop scattering with the residual nuclear polarization, leading to an increased  $|I|$ .

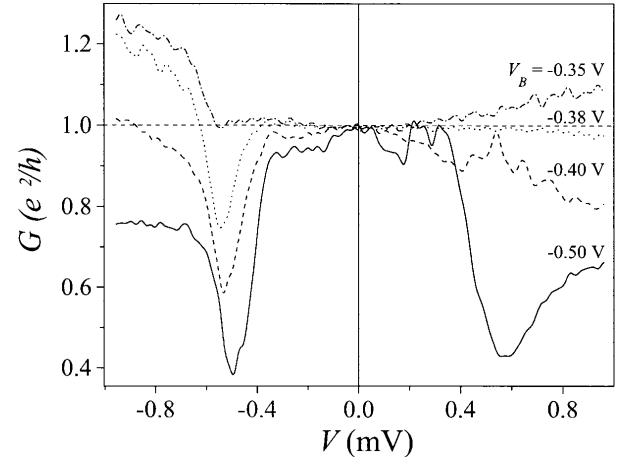


FIG. 6. Plots of the differential conductance through the  $AB$  split gate as a function of  $V$  for various values of  $V_B$ . The bulk filling factor  $\nu=2$ , and  $V_A = -1$  V. When gate  $B$  is only partially depleted (e.g.,  $V_B = -0.35$  V), but still transmitting only one edge state, the conductance is basically flat at  $e^2/h$ , with a slight rise at nonlinear biases. When gate  $B$  is depleted ( $V_B < -0.35$  V), the conductance deviates dramatically from  $e^2/h$ .

We refer the reader to Ref. 18 for a detailed explanation.

In our more recent measurements (e.g., Fig. 3), the hysteresis was observed to be antisymmetric.  $I$  is enhanced when sweeping  $V$  away from zero for positive  $V$  (because the spin gap is smaller due to the spin-up polarization), but suppressed for negative  $V$  (because the spin gap is larger due to the spin-down polarization). The hysteresis sweeps out a figure-eight (antisymmetric) rather than a pinched loop (symmetric). This asymmetric hysteresis is most naturally interpreted in terms of the nuclear Zeeman effect, as discussed in Sec. III.

Why is the hysteresis symmetry different? The answer lies in the gate voltages applied to the quantum point contacts (QPC's) that were used to inject polarized electrons into the scattering region. We observed antisymmetric hysteresis when we only partially depleted gates  $B$  and  $C$ , as shown in Fig. 1(a). Upon increasing the voltage on these gates so that they became fully depleted, the hysteresis became symmetric. In the experiments of Ref. 18, fully depleted QPC's were used, resulting in symmetric hysteresis.

This observation led us to examine the  $AB$  split gate by itself, in various states of depletion, to try to understand what was causing this hysteresis change. Figure 6 shows the differential conductance through the  $AB$  split gate as a function of  $V$  for various values of  $V_B$ , with  $V_A$  held at  $-1$  V. For  $V_B > -0.35$  V, the conductance is a fairly flat  $e^2/h$ , with some deviation at large negative  $V$ . For more negative values of  $V_B$ , however, the conductance deviates drastically from  $e^2/h$  for  $|V| > 0.4$  mV. The value of the gate voltage  $V_B$  at which this transition occurs is at the voltage at which the electron gas becomes fully depleted under the gate itself.

Consider the paths of the edge channels near the  $AB$  split gate, diagrammed in Fig. 7. The edge channels entering the split gate from above are populated to the potential  $\mu = -eV$ , while the edge channels entering from the bottom are at zero potential. If the  $AB$  split gate forms a fully depleted QPC, the incoming and outgoing outer edge channels

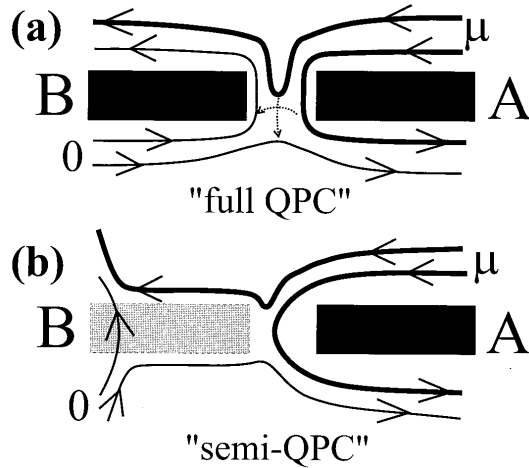


FIG. 7. Schematic of full and semi-QPC's, with the edge states flowing in the directions indicated by the arrows, and labeled by their electrochemical potentials. In (a), both arms of the QPC are fully depleted. The incoming and outgoing edge channels are forced to run close to each other inside the QPC, so if there is a large difference in their potentials, a large electric field exists within the QPC, which would distort the potential profile and cause unintended scattering and edge-state mixing (dotted arrows). In (b), gate  $B$  is partially depleted, but still only transmits one edge state, and the inner edge state is prevented from leaking through the region between the split gates by a large  $V_A$ . The incoming and outgoing edge channels are now far apart, preventing the scattering problems in (a).

pass very close to each other while making their way between the gates, as shown in Fig. 7(a). If the bias  $V$  is high, a large electric field will exist within the QPC, which could cause the electrostatic potential profile near the constriction to be deformed and cause unintended scattering and edge-state mixing (dotted lines). For a partially depleted QPC, shown in 7(b), the edge states are very far apart, and little scattering is expected to occur.

We therefore conclude that the electrons transmitted through a fully depleted QPC [Fig. 7(a)] at high biases exhibit significant interchannel scattering and thus are (a) not spin polarized and (b) not populated up to the electrochemical potential  $\mu$  at which they entered the QPC. On the other hand, for a partially depleted QPC [Fig. 7(b)], the edge channels of different potentials remain macroscopically apart from each other, preserving the nonequilibrium current distribution even at large nonlinear biases. As a result, the mea-

surements and interpretations reported in Sec. III, using partially depleted QPC's, are more reliable than those given in Ref. 18, where fully depleted QPC's were employed.

Although we have shown that a full QPC displays complex behavior under high bias, the connection between this behavior and the change in the hysteresis loop remains poorly understood. This is because the detailed behavior of the individual QPC's in this limit is not known; more experimental and theoretical work is required. It should be possible to empirically measure the scattering matrix of such a QPC as a function of  $V$  and the gate voltages, but we have not made an attempt to do so. Further, theoretical models of QPC's under high bias that take into account the distortion of the electrostatic potential profile mentioned above should be developed.

## VI. CONCLUSIONS

We have observed  $I$ - $V$  asymmetry in scattering between spin-polarized edge states, and detected remarkably strong effects of GaAs nuclear spins upon these  $I$ - $V$  traces. For forward bias, the  $I$ - $V$  trace displays a threshold which is nearly the bare Zeeman splitting, and for reverse bias the current increases only gradually with no apparent threshold. We also observed hysteresis in these traces, which we interpret as being due to a combination of the dynamic nuclear polarization of the nearby nuclei and the hyperfine influence of the nuclear polarization on the electron energies. The strength of the Overhauser field created by the polarized nuclei was found to be nearly as large as the external field itself. The evidence for nuclear influence was supported by a series of NMR sweeps, which demonstrated that NMR absorption affected the current flow through the device. From these experiments, we conclude that it is critical to consider the hyperfine interaction between Ga and As nuclei and the 2DEG in these systems, and that these interactions may be useful as a local probe of the edge.

## ACKNOWLEDGMENTS

We wish to thank Leo Kouwenhoven for useful discussions, and Bruce Kane and Jeff Beeman for technical assistance. This work was supported by the Director, Office of Energy Research, Office of Basic Energy Sciences, Division of Materials Sciences, of the U.S. Department of Energy under Contract No. DE-AC03-76SF00098. M.R.M. acknowledges support from the NSF MRSEC for Technology Enabling Heterostructures Grant No. DMR-9400415.

<sup>1</sup>For a review, see *The Quantum Hall Effect*, edited by R. E. Prange and S. M. Girvin (Springer, New York, 1990).

<sup>2</sup>S. L. Sondhi, A. Karlhede, S. A. Kivelson, and E. H. Rezayi, *Phys. Rev. B* **47**, 16 419 (1993).

<sup>3</sup>S. E. Barrett, G. Dabbagh, L. N. Pfeiffer, K. W. West, and R. Tycko, *Phys. Rev. Lett.* **74**, 5112 (1995).

<sup>4</sup>A. Schmeller, J. P. Eisenstein, L. N. Pfeiffer, and K. W. West, *Phys. Rev. Lett.* **75**, 4290 (1995); E. H. Aifer, B. B. Goldberg, and D. A. Broido, *ibid.* **76**, 680 (1996).

<sup>5</sup>M. Dohers, K. v. Klitzing, J. Schneider, G. Weimann, and K. Ploog, *Phys. Rev. Lett.* **61**, 1650 (1988); A. Berg, M. Dohers, R. R. Gerhardts, and K. v. Klitzing, *ibid.* **64**, 2563 (1990).

<sup>6</sup>For a review, see R. J. Hang, *Semicond. Sci. Technol.* **8**, 131 (1993).

<sup>7</sup>A. M. Chang, *Solid State Commun.* **74**, 271 (1990); C. W. J. Beenakker, *Phys. Rev. Lett.* **64**, 216 (1990).

<sup>8</sup>P. L. McEuen, E. B. Foxman, Jari Kinaret, U. Meirav, M. A. Kastner, Ned S. Wingreen, and S. J. Wind, *Phys. Rev. B* **45**,

- 11 419 (1992); P. L. McEuen, N. S. Wingreen, E. B. Foxman, J. Kinaret, U. Meirav, M. A. Kastner, Y. Meir, and S. J. Wind, *Physica B* **189**, 70 (1993).
- <sup>9</sup>D. B. Chklovskii, B. I. Shklovskii, and L. I. Glazman, *Phys. Rev. B* **46**, 4026 (1992).
- <sup>10</sup>N. B. Zhitenev, R. J. Haug, K. v. Klitzing, and K. Eberl, *Phys. Rev. Lett.* **71**, 2292 (1993).
- <sup>11</sup>S. W. Hwang, D. C. Tsui, and M. Shayegan, *Phys. Rev. B* **48**, 8161 (1993); S. Takaoka, K. Oto, H. Kurimoto, K. Murase, K. Gamo, and S. Nishi, *Phys. Rev. Lett.* **72**, 3080 (1994); R. J. F. van Haren, F. A. P. Blom, and J. H. Wolter, *ibid.* **74**, 1198 (1995).
- <sup>12</sup>A. Karlhede, S. A. Kivelson, K. Lejnell, and S. L. Sondhi, *Phys. Rev. Lett.* **77**, 2061 (1996).
- <sup>13</sup>B. J. van Wees, L. P. Kouwenhoven, E. M. M. Willems, C. J. P. M. Harmans, J. E. Mooij, H. van Houten, C. W. J. Beenakker, J. G. Williamson, and C. T. Foxon, *Phys. Rev. B* **43**, 12 431 (1991), and references therein.
- <sup>14</sup>See, for example, B. W. Alphenaar, P. L. McEuen, R. G. Wheeler, and R. N. Sacks, *Phys. Rev. Lett.* **64**, 677 (1990).
- <sup>15</sup>G. Müller, D. Weiss, A. V. Khaetskii, K. v. Klitzing, S. Koch, H. Nickel, W. Schlapp, and R. Lösch, *Phys. Rev. B* **45**, 3932 (1992); A. V. Khaetskii, *ibid.* **45**, 13 777 (1992); Y. Takagaki, K. J. Friedland, J. Herfort, H. Kostial, and K. Ploog, *ibid.* **50**, 4456 (1994).
- <sup>16</sup>S. Komiyama, H. Hirai, M. Ohsawa, Y. Matsuda, S. Sasa, and T. Fujii, *Phys. Rev. B* **45**, 11 085 (1992).
- <sup>17</sup>B. E. Kane, L. N. Pfeiffer, and K. W. West, *Surf. Sci.* **305**, 176 (1994); *Phys. Rev. B* **46**, 7264 (1992).
- <sup>18</sup>Keith R. Wald, Leo P. Kouwenhoven, Paul L. McEuen, Nijs van der Vaart, and C. T. Foxon, *Phys. Rev. Lett.* **73**, 1011 (1994).
- <sup>19</sup>N. B. Zhitenev, R. J. Haug, K. v. Klitzing, and K. Eberl, *Europhys. Lett.* **28**, 121 (1994). This reference considers scattering between orbital LL edge states (spin degenerate), but we believe their model is applicable to spin-split edge states, with the Zeeman splitting taking the place of the LL orbital energy splitting in their Eq. (1).
- <sup>20</sup>B. E. Kane *et al.*, *Phys. Rev. Lett.* **61**, 1123 (1988).
- <sup>21</sup>N. B. Zhitenev, R. J. Huag, K. v. Klitzing, and K. Eberl, *Phys. Rev. B* **51**, 17 820 (1995).
- <sup>22</sup>I. D. Vagner and T. Maniv, *Physica B* **204**, 141 (1995).
- <sup>23</sup>The current equilibration typically displays exponential decay after an initial period (a few seconds) of super exponential decay. A detailed treatment can be found in Keith Wald, Ph.D thesis, University of California at Berkeley, 1995.
- <sup>24</sup>M. Krapf, G. Denninger, H. Pascher, G. Weimann, and W. Schlapp, *Solid State Commun.* **78**, 459 (1991).
- <sup>25</sup>The nuclear spin for all the relevant Ga and As isotopes is 3/2, so a ‘‘flop’’ process involves changing  $I_z$  by  $\pm \frac{1}{2}$  on its spin ladder.
- <sup>26</sup>A. Usher, R. J. Nicholas, J. J. Harris, and C. T. Foxon, *Phys. Rev. B* **41**, 1129 (1990).
- <sup>27</sup>D. Paget, G. Lampel, B. Sapoval, and V. S. Safarov, *Phys. Rev. B* **15**, 5780 (1977).
- <sup>28</sup>Our measured resonance frequencies differ by a few percent from the commonly observed values [see *CRC Handbook of Chemistry and Physics* (CRC Press, Boca Raton, FL, 1989), Vol. 69, p. E-81], probably because the magnet was not accurately calibrated.
- <sup>29</sup>See, for example, R. Tycko, S. E. Barrett, G. Dabbagh, L. N. Pfeiffer, and K. W. West, *Science* **268**, 1460 (1995).
- <sup>30</sup>P. L. McEuen, D. Dixon, K. Wald, and M. R. Melloch, *Proceedings of Correlated Fermions and Transport in Mesoscopic Systems - Moriond Conference, 1996* (Editions Frontiers, Gif-Sur-Yvette Cedex, France, 1996).
- <sup>31</sup>Lex Rijkels and Gerrit E. W. Bauer, *Phys. Rev. B* **50**, 8629 (1994).
- <sup>32</sup>The measurement setup in Ref. 18 had the ground and the current amplifier reversed compared to our setup [Fig. 1(a)], so the measured current consisted of electrons which had not been scattered.